Original Article
Body part classification of CT images using a gradient boosting decision tree

Cheng-Long Liu[1,2], Ying-Ying Shi[3], Cui-Yun Yuan[4], Shu-Yun Chen[5], Wen-Xian Peng[2], Pei-Zhong He[2]

[1]University of Shanghai for Science and Technology, Shanghai, China; [2]Shanghai University of Medicine and Health Sciences, Shanghai, China; [3]Affiliated Hangzhou First People's Hospital, Zhejiang University School of Medicine, Hangzhou, China; [4]Cancer Hospital Chinese Academy of Medical Sciences, Shenzhen Center, Shenzhen, China; [5]Ruian People's Hospital, Ruian, China

Abstract: Background: The automatic classification of five body parts based on computed tomography (CT) images is a critical preprocessing step in many computer-aided diagnostic systems because the body's different organs have highly diverse features. Machine learning has made remarkable progress in the field of medical image processing. Methods: We established a gradient boosting decision tree (GBDT) machine-learning algorithm using statistical features, stochastic-model-based features, and signal-processing-based features for the discrimination of five body parts including the head, the chest, the abdomen, the pelvis, and the four limbs based on CT images. 83,714 CT images were included in this study. The textural features were extracted and normalized. After that, a logistic regression analysis and a Pearson correlation analysis were implemented for the feature selection to enhance the robustness of the model. A GBDT algorithm with a 10-fold cross validation strategy was applied to the classification based on the selected optimal feature group. Results: The proposed method achieved consistent best performance in terms of accuracy (ACC), sensitivity (SEN), specificity (SPE), positive predicted value (PPV), negative predicted value (NPV), and F1-scores. It is noteworthy that the accuracy of GBDT for differentiating the five body parts is greater than 99%, which outperforms other state-of-the-art models. Conclusion: The proposed approach is effective at distinguishing the five body parts and has superior diagnostic performance compared with existing computer-aided diagnostic methods. It provides a timesaving and robust classification method for radiologists and researchers.

Keywords: Body parts, textual features, machine learning, computed tomography

Introduction

In recent years, with the development of artificial intelligence, more and more automatic image analysis algorithms have been developed to help clinicians interpret and evaluate radiological images. Among all the radiological images, CT is one of the most common forms of medical imaging scans. Since different organs have highly different characteristics, CT image analysis algorithms are generally integrated with prior knowledge such as nodule diameters to identify and analyze specific lesions or organs [1-3]. If those algorithms were randomly applied to data sets containing irrelevant medical images, it would be rather time-consuming and would most likely reduce the accuracy of the classification results.

In real-world clinical workflows, CT image recognition regularly relies on digital imaging and communications in medicine (DICOM) tag information, which is occasionally unreliable. Furthermore, in international cooperative research projects, due to the use of multiple languages and the non-uniform abbreviations of DICOM tags, it seems to be unrealistic to effectively classify medical images based on DICOM tag information [4]. Manual classification is an alternative approach, but it is not practicable for large datasets.

However, compared with the extensive investigated organ segmentation [5, 6] and cancer classification [7, 8] methods, the automatic identification of five body parts including the head, the chest, the abdomen, the pelvis, and
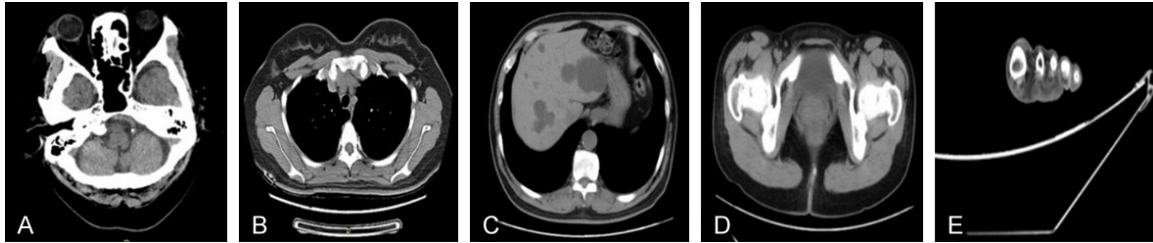
Figure 1. CT images of the five body parts. (A-E) represents the head, the chest, the abdomen, the pelvis, and the four limbs (a foot in the figure) respectively.
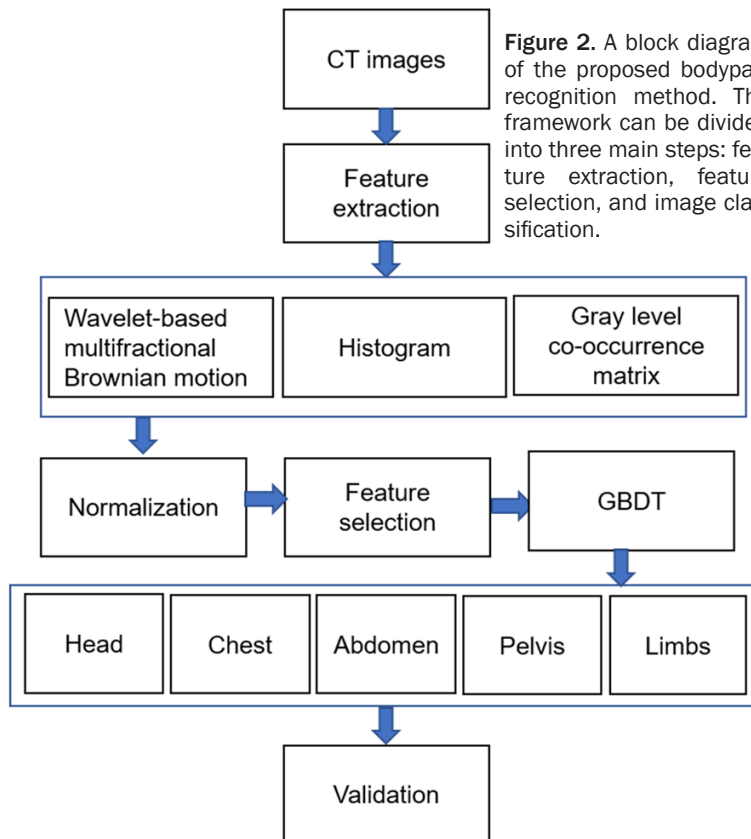

Figure 2. A block diagram of the proposed bodypart recognition method. The framework can be divided into three main steps: feature extraction, feature selection, and image classification.

the limbs (the ankles, wrists, knees, elbows, and feet are included with the limbs) in medical images is still less explored. To tackle this problem, we designed a machine-learning classification method using histograms, gray level co-occurrence matrixes, and wavelet-transform-based Brownian fractal model features to classify five body parts in CT images.

Materials and methods

Clinical data

This study was approved by the institutional review boards of Affiliated Hangzhou First People's Hospital, Zhejiang University School of Medicine. The requirement for written informed consent from patients was waived.

A total of 83,714 CT images were retrospectively collected from Affiliated Hangzhou First People's Hospital, Zhejiang University School of Medicine from 2016 to 2019 with very different ages (20-80 years old, median: 49.5). Of the 83,714 CT scans, 2,895, 20,837, 7,597, 13,946, and 38,439 were head, chest, abdomen, pelvis, and limbs images, respectively. All the unenhanced and enhanced CT scans were obtained from the Siemens Sensation 16-layer spiral CT (Siemens, Erlangen, Germany). The image format was Digital Imaging and Communications in Medicine (DICOM). The scan parameters were: tube voltage 120 kV; tube current automatic regulation; 1-2 millimeters cross-sectional thickness; 1-2 millimeters cross-sectional distance; scan pitch 1.3; and 16×0.625 millimeters collimation. **Figure 1** shows samples of five body part CT images from the enrolled dataset.

Overview of the proposed methodology

A novel gradient boosting decision tree (GBDT) using statistical features, stochastic-model-based features, and signal-processing-based features for developing CT image classification of five body parts is presented. A block diagram of the proposed body part recognition strategy is delineated in **Figure 2**. After all the clinical data was collected, a feature extraction algo-

Table 1. Textural features

Feature groups	Descriptions
Histogram	1. Standard deviation; 2. Skewness; 3. Mean intensity; 4. Entropy; 5. Kurtosis; 6. Uniformity
GLCM	7. Angular second moment; 8. Correlation; 9. Contrast; 10. Sum average; 11. Entropy; 12. Sum variance; 13. Inverse difference moment; 14. Variance; 15. Difference variance; 16. Sum entropy; 17. Difference entropy; 18. Information Measures of Correlation (1); 19. Information Measures of Correlation (2)
Wavelet-based multifractional Brownian motion	20. Approximation coefficients-based fractal dimension; 21. Horizontal details-based fractal dimension; 22. Vertical details-based fractal dimension; 23. Diagonal details-based fractal dimension

rithm was utilized to extract the 23 texture features from the CT images of the five body parts, including 6 histogram texture features, 13 gray level co-occurrence matrix (GLCM) texture features, and 4 wavelet-based multifractional Brownian motion texture features. In the next step, a multiple logistic regression analysis and a Pearson correlation analysis were implemented to select the optimal features from the high dimensional features (23 features) to enhance the classification performance. Finally, the GBDT algorithm was adopted as the classifier based on the selected features while three other classifiers, including Support Vector Machine (SVM), K-nearest Neighbor (KNN), and Gaussian Discriminant Analysis (GDA) were processed for comparison. Eventually, the performances of the four classifiers were evaluated in terms of their ACC, SEN, SPE, PPV, NPV, and F1-scores.

Feature extraction

Feature extraction methods can be divided into five major subsets: (1) a statistical approach, (2) a structural approach, (3) a model-based stochastic approach, (4) a morphology-based approach, and (5) a signal processing approach. In our research, three fundamental feature extraction approaches including the statistical method, the model-based stochastic method, and the signal processing methods were evaluated. It is noteworthy that the model-based stochastic method and the signal processing method were assembled to calculate the required features.

The statistical methods generate parameters to represent the randomness of the image gray spatial distribution, among which GLCM is one of the most commonly-used approaches. GLCM considers the statistical and spatial relationship of the pixels in the image. It is created by calculating how often pairs of pixels with spe-

cific values and in a specified spatial relationship occur in an image [9]. Then 13 statistical texture features are extracted based on the grey level co-occurrence matrix. In addition, the histological characteristics of the five parts of the body can be well reflected in the gray scale model, and a histogram is an intuitive statistical method of gray scale modeling [10].

Wavelet transform, which is a typical signal processing method based on a multi-scale analysis including time domain and frequency domain analysis, combined with multi-fractional Brownian motion, which is a representative model-based stochastic method in the spatial domain, had been wildly applied for medical image classification [11-13]. Furthermore, studies show that the combined method of frequency domain and spatial domain produces better features that lead to a stable and robust performance [14-16]. Consequently, four multi-fractal dimension features were calculated based on the Daubechies wavelet filter with four different coefficients: approximation coefficients, horizontal detail coefficients, vertical detail coefficients, and diagonal detail coefficients.

Thus, 23 textural features were extracted from the CT images of the five body parts and included 6 histogram features, 13 GLCM features, and 4 wavelet-based multifractional Brownian motion features, as shown in **Table 1**. Normalization is a linear feature transformation that performs specific scaling on the numerical range of the data without changing its data distribution. The features of the different dimensions can be transformed to the same numerical magnitude, reducing the impact of the features with large variances and eliminating data redundancy and undesirable characteristics. Therefore, to accelerate the speed of the proposed algorithm, all the obtained texture feature data were normalized to [0, 1]. The normalization equation (1) is as follows:

$$X^* = (X-X_{min})/(X_{max}-X_{min}) \tag{1}$$

Where X indicates the original data of the N_{th} dimension, X_{min} represents the minimum value of all the Xs, X_{max} indicates the maximum value of all the Xs, and X^* is the normalized data X.

Feature selection

High dimensional features can reduce the classification accuracy and cause over-fitting. Fortunately, feature selection is a promising method to solve these problems. Thus, multiple logistic regression analysis, which is a critical feature selection method, combined with Pearson correlation analysis were leveraged to select the optimal feature subset from the original feature set. The Pearson correlation analysis essentially calculates the ratio between the covariance and the standard deviation of each feature and the corresponding label. The formula (2) of the Pearson correlation analysis is as follows:

$$P(x,y) = (\sum xy - (\sum x \sum y/N))/\sqrt{(\sum x^2 - ((\sum x)^2/N))(\sum y^2 - ((\sum y)^2/N))} \tag{2}$$

Where x refers to feature and y represents the corresponding label. N is the total number of features. Multiple logistic regression analysis is applied to the analysis whether the feature is statistically significant, which means whether the output p is smaller than 0.05.

The multiple logistic regression analysis and the Pearson correlation analysis were both performed on SPSS 25.0 software. First, the Pearson correlation analysis was carried out for each feature of the five body parts and an absolute value of a Pearson correlation coefficient greater than 0.3, would be retained for the next step. Then, a multiple logistic regression analysis was conducted on the remaining features. Ultimately, the features with significant differences ($P < 0.05$) were selected as the optimal feature subset for the classification.

Feature classification

A gradient boosting decision tree (GBDT) [17] is one of the most powerful machine learning algorithms for building predictive models, as it can superbly demonstrate the real distribution of the data. GBDT was proved to achieve state-of-the-art performance in multi-class classification due to its stability, accuracy, and interpretability [18, 19]. In the case of GBDT, decision tree algorithms taken as weak learners were sequentially boosted to become a strong learner. Each weak learner attempts to minimize the residuals from the previous stage, which improves the efficiency and accuracy of the model. The final strong classification model is achieved by majority vote of the weak learners' results. A logarithmic loss function is applied to calculate the residuals. Finally, the model can be described as shown in the equation (3):

$$F_m(x) = \sum_{m=1}^{M} T(x;\theta_m) \tag{3}$$

Where M represents the training iteration. Each iteration produces a weak classifier $T(x;\theta_m)$. The loss function of the weak classifier is shown in the equation (4):

$$\hat{\theta}_m = arg\theta_m min\sum_{i=1}^{N} L(y_i, F_{m-1}(x_i) + T(x_i;\theta_m)) \tag{4}$$

Where $F_{m-1}(x)$ represents the current model. GBDT determines the parameters of the next weak learner using empirical risk minimization. For classification tasks, L represents logarithmic loss function. The complete training process of GBDT is shown in **Figure 3**.

Thus, the selected optimal feature subset was input to GBDT for classification with a 10-fold cross-validation strategy. For comparison with the performance of GBDT, three other machine learning algorithms including SVM [20], KNN [21], and GDA [22] were implemented based on the same feature set.

Performance analysis

The proposed five body part classification model and three other classifiers were assessed by calculating the parameters of the ACC, SEN, SPE, PPV, NPV, and F1-scores. The calculation equations (5)-(10) of the six evaluation indexes are as follows:

$$ACC = (TP + TN)/(TP + TN + FP + FN) \tag{5}$$

$$SEN = Recall = TP/(TP + FN) \tag{6}$$

$$SPE = TN/(TN + FP) \tag{7}$$

$$PPV = Precision = TP/(TP + FP) \tag{8}$$

$$NPV = TN/(TN + FN) \tag{9}$$

$$F1score = (2 \times Precision \times Recall)/(Precision + Recall) \tag{10}$$
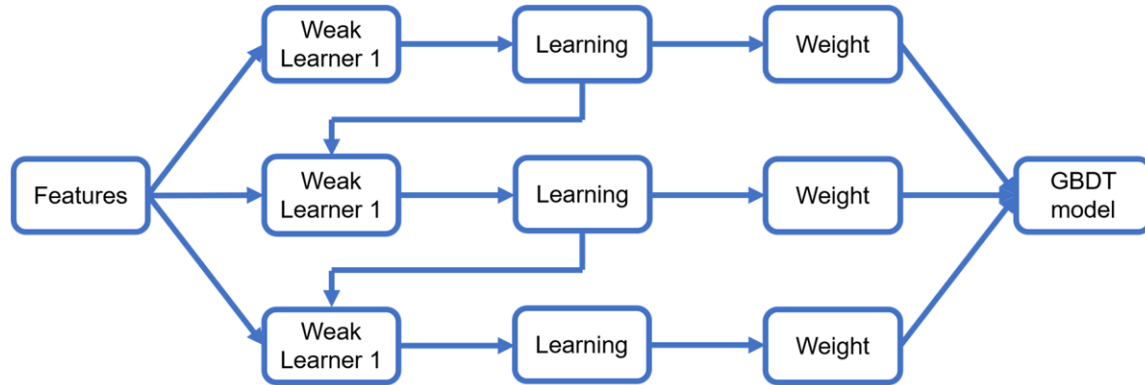
Figure 3. The GBDT training process.

Table 2. Feature selection using logistic regression and Pearson correlation analyses

Feature number	PCC	p value	Feature number	PCC	p value
1	0.588	0.000	13	-0.186	0.000
2	-0.518	0.000	14	-0.201	0.000
3	0.412	0.000	15	0.357	0.000
4	-0.018	0.614	16	0.175	0.000
5	-0.630	0.000	17	0.205	0.000
6	0.325	0.000	18	0.135	0.000
7	-0.025	0.493	19	0.030	0.410
8	0.092	0.012	20	0.373	0.000
9	0.357	0.000	21	0.019	0.603
10	-0.206	0.000	22	0.497	0.000
11	0.212	0.000	23	-0.210	0.000
12	-0.230	0.000			

Notes: Feature numbers are based on **Table 1**.

Where TP is the number of correctly-classified positive samples; TN: the number of correctly-classified negative samples, FP: the number of wrongly-classified positive samples, FN: the number of wrongly-classified negative samples. For the multi-class prediction tasks, if one category is regarded as a positive class, the other categories are considered a negative class automatically. For example, in our research, if the head is taken as a positive class, then the abdomen, chest, pelvis, and limbs are regarded as a negative class.

Results

Results of the feature selection

After our feature selection based on the logistic regression analysis and Pearson correlation

analysis, nine features with both the absolute value of the Pearson correlation coefficient greater than 0.3 and $P < 0.05$ were retained out of 23 features as the optimal feature combination for the body parts classification in the next stage, as shown in **Table 2**. Consequently, nine features, including uniformity, mean intensity, standard deviation, kurtosis, skewness, contrast, difference variance, approximation coefficients-based fractal dimension, and vertical details-based fractal dimension were selected for the classification.

Classification performance comparisons of the four different methodologies

After the feature selection, the optimal feature subgroup was fed into four machine-learning algorithms for classification. As shown in **Table 3**, all the models were estimated in terms of the ACC, SEN, SPE, PPV, NPV, and F1-scores. We observed that the proposed method achieved its consistent best performance in general. Besides, only the KNN classifier achieved the highest SPE (99.96%) and PPV (98.79%) for detecting CT images in the head category. It is noteworthy that all the SVM evaluation indexes are slightly smaller than the GBDT indexes are.

Nevertheless, several outliers emerged in **Table 3**. For example, the SEN, PPV, and F1-scores of KNN for distinguishing the abdomen are 69.53%, 80.60%, and 74.66%, respectively,

Table 3. Performance analysis results of the different classifiers

Evaluation index	Classifier	Head	Chest	Abdomen	Pelvis	Limbs
ACC (%)	GDA	99.68	89.06	93.36	93.82	97.99
	KNN	99.83	94.51	95.72	95.86	97.68
	SVM	99.83	99.20	99.83	99.47	99.41
	GBDT	**99.91**	**99.55**	**99.86**	**99.74**	**99.72**
SEN (%)	GDA	96.23	60.00	93.46	93.75	96.02
	KNN	96.23	95.88	69.53	80.88	97.61
	SVM	99.31	99.35	98.46	98.25	98.89
	GBDT	**99.79**	**99.80**	98.60	**99.21**	**99.22**
SPE (%)	GDA	99.80	98.69	92.25	93.83	99.66
	KNN	**99.96**	94.06	98.33	98.85	97.73
	SVM	99.85	99.16	99.97	99.71	99.86
	GBDT	99.92	**99.46**	**99.98**	**99.85**	**99.95**
PPV (%)	GDA	94.54	93.80	54.63	75.23	99.59
	KNN	**98.79**	84.25	80.60	93.36	97.34
	SVM	95.90	97.50	99.67	98.57	99.83
	GBDT	97.73	**98.41**	**99.83**	**99.23**	**99.89**
NPV (%)	GDA	99.86	88.16	99.30	98.68	96.72
	KNN	99.87	98.57	97.00	96.28	97.97
	SVM	99.96	99.78	99.85	99.65	99.07
	GBDT	**99.99**	**99.93**	**99.86**	**99.84**	**99.64**
F1-score (%)	GDA	95.38	73.19	68.96	83.48	97.77
	KNN	97.50	89.69	74.66	86.67	97.47
	SVM	97.57	98.42	99.06	98.41	99.36
	GBDT	**98.75**	**99.10**	**99.20**	**99.22**	**99.55**

Notes: The best results are marked in bold black.

which are approximately 10-20% smaller than those of the other body parts based on the KNN algorithm are.

Discussion

KNN is a suitable machine-learning algorithm for multiple classification tasks, as it classifies the different categories according to the distance of the samples. To be more specific, an object is more likely to be assigned to the majority class of its k nearest neighbors [23]. Normally, k is manually set as a relatively small integer but one larger than zero. However, a data imbalance exits in the collected five body part CT images. For instance, 7,597 abdomen CT images were included in the dataset, and the number of chest CT images was 20,837, which is almost 3 times the number of abdomen images. It seriously affected the classification performance of the model. **Table 3** substantiates that the classification evaluation indexes (especially the aforementioned SEN,

PPV, and F1-scores in the Results section) of the abdomen were significantly less than the classification evaluation indexes of the other body parts.

It is empirically assumed that feature data obeys a Gaussian distribution, and the classification results obey a Bernoulli distribution simultaneously before and after it is applied to the classification evaluation indexes GDA algorithm [24]. In this way, GDA can produce a satisfied performance. However, according to the classification results, it is likely that the provided dataset does not meet the criteria. SVM is a popular supervised machine model, and it can effectively solve both linear and nonlinear problems particularly with small samples. The principle of the SVM algorithm is to divide the dataset into different classes by creating a line or a hyperplane [25]. As revealed in **Table 3**, even though the dataset applied in this study is considerably large, SVM still gained a surprisingly appreciable performance. However, it consumed 711.57 seconds while the GBDT algorithm only takes 27.38 seconds. In conclusion, our proposed GBDT classifier outperforms other classifiers.

Roth et al. proposed a deep convolutional network for automatically classifying human anatomy images, including the neck, lungs, liver, pelvis, and legs based on CT images [26]. The classification error rate decreased to 5.9% after the data augmentation, and the AUC of the model was 99.8%. Márton et al. evaluated the Random Forest machine learning classifier using a 2-dimensional global shape feature extraction algorithm called the Zernike transform based on three-dimensional magnetic resonance images to detect the head, the chest, the abdomen, the pelvis, and the legs [27]. Principal Component Analysis (PCA) was processed for the feature optimization. The

overall accuracy of their proposed method was 91.5%. Yan et al. developed a multi-instance deep learning algorithm for body part recognition based on a convolutional neural network (CNN) [28]. The framework consists of two stages for discovering the discriminative local regions and identifying the body parts based on these local patches, respectively. Their method achieved the overall classification recall, precision, and F1-scores of 92.21%, 92.25% and 92.23%, respectively. Furthermore, the highest F1-score was up to 98.99% for identifying the femur head while the F1-scores for identifying the neck, clavicle/lung apex, sternal, liver upper, liver middle and abdomen/kidney are all lower than 90%. Min et al. proposed a fast radial basis function artificial neural network algorithm for the classification of the liver and kidneys in the magnetic resonance images [29]. The highest prediction accuracy and standard deviation of their proposed method is 0.9552±0.0066. Gabriel et al. predicted the location of 11 organs (including the lungs, kidney, and liver) using a single multi-label ConvNet for each orthogonal view (axial, coronal, and sagittal) [30]. They obtained an average wall distance of 3.20±7.33 mm, while the human observer achieved 1.23±3.39 mm. Tao et al. proposed a multi-task learning model integrated with an optimized false positive filtering algorithm and a dynamic threshold selection strategy to segment the organs on the TAOWCH and SegTHOR datasets [31]. The results demonstrate that their method gained a better performance than the basic encoder-decoder networks. Compared with all those methods, our proposed GBDT machine learning classification algorithm based on statistics texture features and Wavelet-based multifractional Brownian motion features for differentiating the five body parts achieved ACC, SEN, SPE, PPV, NPV, and F1-scores larger than 99%, which outperformed the discussed state-of-the-art models.

Limitations of this study: First, a data imbalance still exists in our study. The insufficient number of head and abdomen CT images decreased the reliability and portability of the model. Second, the algorithm requires high computational performance, and the model is relatively time-consuming. More CT images will be collected for further research and the framework will be extended for three-dimensional medical images.

Conclusion

A machine-learning classification method for five body parts, including the head, the chest, the abdomen, the pelvis, and the limbs using a novel gradient boosting decision tree (GBDT) based on statistical features, stochastic-model-based features, and signal-processing-based features is proposed. The results empirically demonstrate that the proposed classification model can accurately and stably identify the five body parts.

Acknowledgements

Disclosure of conflict of interest

None.

Address correspondence to: Pei-Zhong He, College of Medical Imaging, Shanghai University of Medicine and Health Sciences, Zhoupu Town, Pudong New Area, Shanghai 201318, China. Tel: +86-13023296316; E-mail: hepz@sumhs.edu.cn; Wen-Xian Peng, College of Medical Imaging, Shanghai University of Medicine and Health Sciences, Shanghai 201318, China. Tel: +86-18805712978; E-mail: pengwx@sumhs.edu.cn

References

[1] Liu T, Guo Q, Lian C, Ren X, Liang S, Yu J, Niu L, Sun W and Shen D. Automated detection and classification of thyroid nodules in ultrasound images using clinical-knowledge-guided convolutional neural networks. Med Image Anal 2019; 58: 101555.

[2] Qi LL, Wu BT, Tang W, Zhou LN, Huang Y, Zhao SJ, Liu L, Li M, Zhang L, Feng SC, Hou DH, Zhou Z, Li XL, Wang YZ, Wu N and Wang JW. Long-term follow-up of persistent pulmonary pure ground-glass nodules with deep learning-assisted nodule segmentation. Eur Radiol 2020; 30: 744-755.

[3] Wang S, He K, Nie D, Zhou S, Gao Y and Shen D. CT male pelvic organ segmentation using fully convolutional networks with boundary

sensitive representation. Med Image Anal 2019; 54: 168-178.

[4] Dicken V, Lindow B, Bornemann L, Drexl J, Nikoubashman A and Peitgen HO. Rapid image recognition of body parts scanned in computed tomography datasets. Int J Comput Assist Radiol Surg 2010; 5: 527-535.

[5] Wang S, He K, Nie D, Zhou S, Gao Y and Shen D. CT male pelvic organ segmentation using fully convolutional networks with boundary sensitive representation. Med Image Anal 2019; 54: 168-178.

[6] Wang S, Nie D, Qu L, Shao Y, Lian J, Wang Q and Shen D. CT male pelvic organ segmentation via hybrid loss network with incomplete annotation. IEEE Trans Med Imaging 2020; 39: 2151-2162.

[7] Masood A, Sheng B, Yang P, Li P, Li H, Kim J and Feng DD. Automated decision support system for lung cancer detection and classification via enhanced rfcn with multilayer fusion RPN. IEEE Trans Industr Inform 2020.

[8] Liu C, Wang X, Liu C, Sun Q and Peng W. Differentiating novel coronavirus pneumonia from general pneumonia based on machine learning. Biomed Eng Online 2020; 19: 66.

[9] Cao K, Xu J and Zhao WQ. Artificial intelligence on diabetic retinopathy diagnosis: an automatic classification method based on grey level co-occurrence matrix and naive Bayesian model. Int J Ophthalmol 2019; 12: 1158-1162.

[10] Gihr GA, Horvath-Rizea D, Hekeler E, Ganslandt O, Henkes H, Hoffmann KT, Scherlach C and Schob S. Histogram analysis of diffusion weighted imaging in low-grade gliomas: in vivo characterization of tumor architecture and corresponding neuropathology. Front Oncol 2020; 10: 206.

[11] Shimizu Y, Barth M, Windischberger C, Moser E and Thurner S. Wavelet-based multifractal analysis of fMRI time series. Neuroimage 2004; 22: 1195-1202.

[12] Zhang MM, Yang H, Jin ZD, Yu JG, Cai ZY and Li ZS. Differential diagnosis of pancreatic cancer from normal tissue with digital imaging processing and pattern recognition based on a support vector machine of EUS images. Gastrointest Endosc 2010; 72: 978-985.

[13] Bhowmick C, Dutta PK and Mahadevappa M. Wavelet transform and texton based analysis for detection of benign and malignant masses. Annu Int Conf IEEE Eng Med Biol Soc 2020; 2020: 2178-2181.

[14] Kaplan LM. Extended fractal analysis for texture classification and segmentation. IEEE Trans Image Process 1999; 8: 1572-1585.

[15] Lopes R, Ayache A, Makni N, Puech P, Villers A, Mordon S and Betrouni N. Prostate cancer characterization on MR images using fractal features. Med Phys 2011; 38: 83-95.

[16] Islam A, Reza SM and Iftekharuddin KM. Multifractal texture estimation for detection and segmentation of brain tumors. IEEE Trans Biomed Eng 2013; 60: 3204-3215.

[17] Friedman JH. Greedy function approximation: a gradient boosting machine. Ann Stat 2001, 29: 1189-1232.

[18] Kuo DE, Wei MM, Armbrust KR, Knickelbein JE, Yeung I, Nussenblatt RB, Chan CC and Sen HN. Gradient boosted decision tree classification of endophthalmitis versus uveitis and lymphoma from aqueous and vitreous IL-6 and IL-10 levels. J Ocul Pharmacol Ther 2017; 33: 319-324.

[19] Zhou S, Wang S, Wu Q, Azim R and Li W. Predicting potential miRNA-disease associations by combining gradient boosting decision tree with logistic regression. Comput Biol Chem 2020; 85: 107200.

[20] Yang CY and Lin CP. Classification of cognitive reserve in healthy older adults based on brain activity using support vector machine. Physiol Meas 2020; 41: 065009.

[21] Abu Alfeilat HA, Hassanat A, Lasassmeh O, Tarawneh AS, Alhasanat MB, Eyal Salman HS and Prasath V. Effects of distance measure choice on K-Nearest neighbor classifier performance: a review. Big Data 2019; 7: 221-248.

[22] Fang C, Li C, Cabrerizo M, Barreto A, Andrian J, Rishe N, Loewenstein D, Duara R and Adjouadi M. Gaussian discriminant analysis for optimal delineation of mild cognitive impairment in Alzheimer's disease. Int J Neural Syst 2018; 28: 1850017.

[23] Ashari A, Paryudi I and Tjoa AM. Performance comparison between naïve bayes, decision tree and k-nearest neighbor in searching alternative design in an energy simulation tool. International Journal of Advanced Computer Science and Applications 2013; 4.

[24] Salvador T, Elies F, Javier V, Pieter W, Howe Franklyn A, Margarida J, Ana-Paula C, Daniel M, Angel M, Jesús P, Griffiths John R, Alan W, Peet Andrew C, Carmen MM, Bernardo C, Carles A and Robles M. Incremental gaussian discriminant analysis based on graybill and deal weighted combination of estimators for brain tumour diagnosis. J Biomed Inform 2011; 44: 677-687.

[25] Noble William S. What is a support vector machine. Nat Biotechnol 2006; 24: 1565-1567.

[26] Roth HR, Lee TY, Shin HC, Seff A and Summers RM. Anatomy-specific classification of medical images using deep convolutional nets. IEEE International Symposium on Biomedical Imaging 2015.

[27] Tóth M, Ruskó L and Csébfalvi B. Automatic recognition of anatomical regions in three-dimensional medical images. Comput Biol Med 2016; 76: 120-133.

[28] Yan Z, Zhan Y, Peng Z, Liao S, Shinagawa Y, Zhang S, Metaxas DN and Zhou XS. Multi-instance deep learning: discover discriminative local anatomies for bodypart recognition. IEEE Trans Med Imaging 2016; 35: 1332-1343.

[29] Xu M, Qian P, Zheng J, Ge H and Muzic RF Jr. A novel radial basis neural network-leveraged fast training method for identifying organs in mr images. Comput Math Methods Med 2020; 2020: 4519483.

[30] Humpire-Mamani GE, Setio A, van Ginneken B, Jacobs C. Efficient organ localization using multi-label convolutional neural networks in thorax-abdomen CT scans. Phys Med Biol 2018; 63: 085003.

[31] He T, Hu J, Song Y, Guo J and Yi Z. Multi-task learning for the segmentation of organs at risk with label dependence. Med Image Anal 2020; 61: 101666.